Published in final edited form as:
Immunity. 2008 December 19; 29(6): 971–985. doi:10.1016/j.immuni.2008.10.015.

Successful interstitial navigation by killer T cells enables efficient anti-tumor immunity

Paulus Mrass[1], **Ichiko Kinjyo**[2], **Lai Guan Ng**[1,3], **Steven L. Reiner**[2], **Ellen Puré**[1,4], and **Wolfgang Weninger**[1,3,5]

[1]The Wistar Institute, Philadelphia, PA 19104, USA

[2]Abramson Family Cancer Research Institute and Department of Medicine, University of Pennsylvania, Philadelphia, PA 19104, USA

[3]The Centenary Institute for Cancer Medicine and Cell Biology, Newtown, NSW 2042, Australia

[4]Ludwig Institute of Cancer Research, Philadelphia, PA 3601, USA

[5]Discipline of Dermatology, University of Sydney, Camperdown NSW 2050, Australia

Summary

A killer T lymphocyte must both seek and destroy transformed cells within cancerous tissue in order to eliminate a tumor. Although lymphocytes are constitutively non-adherent cells, they undergo facultative polarity during migration and upon interaction with cells presenting cognate antigen, suggesting that lymphocyte polarity might be critical for tumor cell rejection. Using two-photon imaging of tumor-infiltrating T lymphocytes, we found that CD44, a receptor for extracellular matrix proteins and glycosaminoglycans, is crucial for interstitial navigation within tumors as well as efficiency of target cell screening. CD44 functions as a critical regulator of intra-tumoral movement by stabilizing cell polarity in migrating T cells. Stable anterior-posterior asymmetry is maintained by CD44 independently of its extracellular domain. Instead, migratory polarity depends on the recruitment of ERM-proteins by the intracellular domain of CD44 to the posterior cellular protrusion. These data provide evidence that facultative polarity mediated by CD44 is a key regulator of killer T cell migration and navigation, and that even moderate disturbances in the ability to seek out transformed cells have profound effects on the capacity to ultimately reject tumors.

Introduction

A key function of the immune system is to protect the organism against transformed tumor cells. Cytotoxic killer T lymphocytes (CTL) are a crucial cell type in this context as they are capable of directly destroying malignant cells. This function of CTL depends critically on their capability to seek and recognize cancer and/or tumor-associated stromal cells that may be located anywhere in the body (Mrass and Weninger, 2006). Thus, CTL must migrate from the blood stream into organs, find their way through the extracellular matrix (ECM)-rich interstitial space and finally interact physically with target cells. Recognition of MHC-peptide (pMHC)

Address for correspondence: Wolfgang Weninger, M.D., The Centenary Institute for Cancer Medicine and Cell Biology, Locked Bag No. 6, Newtown, NSW 2041, Australia, Phone: +61 2 9515 6821, Fax: +61 2 9656 1048, Email: w.weninger@centenary.org.au.

complexes by the T cell receptor (TCR) then leads to the release of cytotoxic mediators and cytokines ultimately resulting in the death of their targets.

Several core activities of T lymphocytes, such as locomotion through tissue stroma and cell-to-cell interactions, are associated with facultative polarity (Krummel and Macara, 2006; Sanchez-Madrid and del Pozo, 1999). Thus, the shape of a crawling T cell is characterized by the formation of a flattened lamellipodium at the leading edge and a small, handle-like protrusion at the rear, the uropod. Chemotactic receptors are enriched at the leading edge, where they may sense chemokine gradients within tissues. In contrast, adhesion molecules, such as CD43, CD44, and ICAMs localize to the uropod of motile T cells. After receiving a migratory stop signal delivered by TCR-pMHC interaction, T lymphocytes change to a more rounded morphology. Nevertheless, certain molecules, such as the TCR, coordinately segregate to the T cell-target cell interface to form the immunologic synapse (IS), while others, such as CD43 move to the distal pole of the cell (Dustin, 2008; Shaw, 2005). In naïve T cells the IS is thought to regulate cellular activation and fate determination, whereas in effector CTL it is involved in the directed secretion of cytotoxic mediators (Chang et al., 2007; Stinchcombe and Griffiths, 2003). T lymphocyte locomotion and target cell interactions have been extensively studied in cell culture, and have revealed common and distinct regulatory cues in the mediation of asymmetry during these activities. For example, PDZ-containing proteins, including the Par3, Crumbs, and Scribble complex, have been implicated in coordinating surface molecule distribution in uropod-containing T lymphocytes and during IS formation (Ludford-Menting et al., 2005). In contrast, MyH9, a non-muscle myosin heavy chain, is required for migration of T cells in vitro, but dispensable for synapse formation in vitro (Jacobelli et al., 2004). However, little is known about the molecular regulation of facultative polarity and consequences of its disruption in T lymphocytes within a physiologic environment.

To gain mechanistic insight into T lymphocyte function in vivo, observation of cells by microscopic means is of great advantage, as this allows direct characterization of molecules involved in interactions with cellular and extracellular components of their specific microenvironment. The need for intravital imaging at high resolution has recently been met by the availability of two-photon microscopy, which has enabled the definition of the basic migratory patterns of lymphocytes in lymphoid and inflammatory tissues (Bousso and Robey, 2004; Cahalan and Parker, 2008; Germain et al., 2006; Halin et al., 2005; Ng et al., 2008). Thus, it has been shown that, in the absence of cognate antigen, naïve and effector T cells in secondary lymphoid and peripheral organs, respectively, are very actively migrating and reveal a polarized shape. Upon antigen encounter, both cell types undergo stable interactions with target cells, such as dendritic cells or tumor cells. Although the molecular cues regulating locomotion of T lymphocytes have been studied in great detail in vitro, it is not yet known how these cells navigate through their respective microenvironments in vivo.

We have previously shown that tumor-infiltrating T lymphocytes (TIL) were in close contact with ECM fibers (Mrass et al., 2006), thereby suggesting the involvement of adhesion receptors in this process. Amongst these molecules is CD44, a cell surface glycoprotein, which is subject to extensive alternative splicing (reviewed in (Ponta et al., 2003; Pure and Cuff, 2001)). The extracellular domain of CD44 can interact with ECM components, including hyaluronic acid (HA), fibronectin, laminin, collagen and osteopontin. CD44 has been implicated in the interactions of freshly activated T cells with blood vessel endothelium (DeGrendele et al., 1997). However, it is unclear whether CD44 is involved in T cell migration outside the vascular system.

Besides the roles of CD44 in T lymphocyte trafficking, the intracellular domain of CD44 contains a number of binding motifs for a variety of signaling molecules implicated in cell shape regulation. For example members of the ezrin, radixin, moesin (ERM) family interact

with CD44 (Turley et al., 2002). In an activated (phosphorylated) state, these molecules act as cross-linkers of the cortical actin filament and cell surface receptors (Bretscher et al., 2002).

Based on the above-described activities of CD44 and its sequestered localization to the uropod of migrating T lymphocytes (Sanchez-Madrid and del Pozo, 1999) we speculated that this molecule might be involved in the regulation of killer T lymphocyte function in vivo. In order to test this hypothesis, we exploited our recently developed two-photon imaging model of intact tumors (Mrass et al., 2006). Our experiments showed that CD44 regulates the navigation of TIL due to the polarity-promoting function of its cytoplasmic domain. Our results formally demonstrate that CTL migration within target sites represents an essential immunologic checkpoint that determines the potency of effector T cell function and is regulated by CD44.

Results

CD44 is dispensable for the differentiation and trafficking of CTL

In order to assess the role of CD44 in TIL function, we made use of transgenic OT-I mice, whose TCR recognizes ovalbumin peptide$_{257\text{-}264}$, crossed to CD44 knockout animals. We first determined whether CD44 deficiency changed the functional properties of $CD8^+$ T cells after antigen priming in vitro. As expected, antigen-activated OT-I cells, but not OT-IxCD44$^{-/-}$ cells, showed high and sustained expression of CD44 (Figure S1A). Other phenotypic characteristics of effector CTL, such as the expression of L-selectin, CD69 and CD25, as well as the production of cytokines, expression of perforin and granzyme B, as well as cell proliferation were not affected by CD44-deficiency (Figures S1B-S1E and data not shown). Also, OT-I and OT-IxCD44$^{-/-}$ CTL induced specific lysis of E.G7-OVA target cells in vitro with similar efficiency (Figure S1F). In addition, CD44 was not required for motility of naïve T cells in intact lymph nodes or on in vitro substrata (Figure S2).

Previous studies have shown that T cells transiently upregulate HA-binding activity after stimulation (DeGrendele et al., 1997; Lesley et al., 1994). Using flow cytometry, we confirmed that cognate peptide activation induced HA-binding activity of OT-I but not OT-IxCD44$^{-/-}$ cells (Figure S3A). However, HA-binding was lost in fully differentiated CTL at day 8 of culture (Figure S3A). Similarly, tumor- and spleen-infiltrating CTL isolated ex vivo did not reveal HA-binding capability (Figure S3B). As a positive control, CTL were preincubated with mAb IRAWB14, which induces HA-binding capacity of CD44 (Lesley et al., 1993). At all time-points, this treatment led to HA-binding of OT-I, but not OT-IxCD44$^{-/-}$ CTL (Figures S3A and S3B). To further exclude the possibility that HA present in culture media masked binding of exogenously added HA in terminally differentiated CTL, we incubated the cells with biotinylated HA-binding protein (HABP). AKR cells transfected with full length CD44 served as a positive control (Figures S4A and S4B). Freshly stimulated, but not fully differentiated OT-I cells bound HABP in a CD44-dependent manner (Figures S4C-S4E). This suggested that CD44 is in an inactive conformation on the surface of fully differentiated CTL. Consistently, adoptively transferred OT-I and OT-IxCD44$^{-/-}$ CTL from day 8 cultures homed to a similar extent into spleen and tumors (Figures S5A-S5C).

CD44 promotes effective navigation of TIL through the intact tumor-microenvironment

The fact that CD44 appeared to be dispensable for effector CTL generation in vitro as well as their accumulation in tumors allowed us to further dissect its function in killer T cell behavior in vivo. We employed our recently developed tumor-imaging model, which enables tracking of fluorescently-tagged TIL in intact tumors (Mrass et al., 2006). When we compared the migratory activity of adoptively transferred OT-I or OT-IxCD44$^{-/-}$ CTL that infiltrated EL4 tumors that lack expression of cognate OVA protein, we noted a migratory defect of CD44-

deficient cells, as evidenced by a reduction of their mean migratory velocity (V_{mean}; OT-I: 7.5 μm min^{-1}, OT-I$xCD44^{-/-}$: 4.9 μm min^{-1}; Figures 1A-1C, Movie S1).

To obtain a more qualitative understanding of the motility defect in the absence of CD44, we plotted the migration tracks of individual cells corresponding to their V_{means} and confinement ratios (defined as the total length of a track divided by the distance between the starting and the end-point of a track). Subdivision of this migration plot yielded four quadrants with distinct migratory properties (Figure 1D). Quadrant 1 contains cells with low V_{mean} and confinement ratio ("low motility" cells). Quadrant 2 contains cells with low V_{mean} and high confinement ratio, corresponding to cells that actively translocate only during certain periods during the observation while also showing substantial periods of immobility ("non-sustained motility"). In quadrant 3, cells exhibit high V_{mean} and high confinement ratios, which is representative of cells with robust migration with only minimal stop-periods ("sustained motility"). Cells in quadrant 4 show, for most of the observation period, active directional migration. However, at some point, they change direction followed by directional migration toward the site of origin reflected by a high velocity and low confinement ratio. CD44-deficient CTL contained an enhanced number of cells in quadrants 1 and 2, but reduced numbers in quadrant 3 and to a lesser degree quadrant 4 (Figure 1E). These results show that CD44 is required for robust migration, which translates into a larger tissue volume that is screened by wildtype as compared to $CD44^{-/-}$ CTL.

We have previously found that TIL migrate randomly within tumors (Mrass et al., 2006). To determine whether CD44-deficiency changed this behavior, we analyzed square root of time versus displacement plots (Cahalan et al., 2002) of cells in quadrant 3, and found that these exhibited random migratory directionality (Figure 1F). This indicates that, regardless of their CD44-status, CTL, at the population level, do not appear to move along apparent, long-range chemokine gradients within the tumor microenvironment.

We next investigated the influence of cognate antigen on the migration of OT-I and OT-I$xCD44^{-/-}$ TIL. We have previously shown that recognition of cognate antigen within target tissue interferes transiently with migration resulting from physical interactions with antigen-bearing tumor-cells. However, to sustain motility for prolonged periods after adoptive transfer, exposure of T cells to cognate antigen within the tumor-tissue is necessary (Mrass et al., 2006). Given that TCR-signaling has a promigratory effect, it was conceivable that signaling via the TCR might overcome the migratory defect of CD44-deficient T cells. However, analysis of the motility of CTL in E.G7-OVA tumors on day 4 after adoptive transfer revealed a similar migratory defect of OT-I x$CD44^{-/-}$ cells as found in EL4 tumors (Figures 1G-1I), demonstrating that the migratory defect could not be rescued by TCR signaling.

Since it could be argued that CD44 wildtype and $CD44^{-/-}$ cells localize to different regions within tumors, and that this resulted in their migratory differences, we performed co-transfer experiments with differentially tagged cells expressing YFP or ECFP. This allowed the simultaneous tracking of OT-I and OT-I$xCD44^{-/-}$ in identical tumor subregions (Figure 2A, Movie S2). Consistently, we found that under these conditions CD44-deficient cells showed significantly reduced V_{means} and migratory characteristics similar to what we observed after single transfer of individual cell populations (Figures 2B-2D), indicating that the reduced motility of $CD44^{-/-}$ cells is not due to accumulation in different areas of the tumor.

To demonstrate that the migratory defect of $CD44^{-/-}$ cells was indeed due to the absence of CD44 and not to other functional differences of $CD44^{-/-}$ cells, we reintroduced full-length CD44 into $CD44^{-/-}$ T cells prior to adoptive transfer. In comparison to control-transduced CTL, CD44-reconstituted cells showed enhanced motility after homing into identical regions in EL4

tumors (Figures 2E-2H, Movie S3). Collectively, we show that CD44 is a direct regulator of the motility of killer T lymphocytes within target tissues.

CD44 regulates the polarity of migrating CTL

To dissect the molecular basis of the promigratory effect of CD44 in effector CTL, we further analyzed the migratory characteristics of wildtype and $CD44^{-/-}$ T cells in an in vitro system. CTL were either placed on top of a collagen gel (Figures 3A-3C, Movie S4) or on immobilized fibronectin (not shown). Wildtype cells migrated effectively on both substrates with a median V_{mean} of 11 and 9.9 μm min^{-1}, respectively. In contrast, CD44-deficient lymphocytes showed significantly reduced V_{means} (collagen: 9 μm min^{-1}, $P<0.0001$; fibronectin: 8.5 μm min^{-1}, $P<0.0001$). We also found an increased proportion of $CD44^{-/-}$ OT-I cells within quadrants 1 and 2 and decreased numbers in quadrant 3 when V_{means} were plotted against the confinement ratio (Figures 3B and 3C). In order to test whether the migratory defect of CD44-deficient cells was due to altered adhesion, we used static adhesion assays. CD44-deficiency did not affect binding to uncoated dishes or fibronectin (Figure 3D). Immobilized type-I collagen did not support adhesion of either CD44-expressing or -deficient CTL, but rather seemed to block residual binding to plastic (Figure 3D). Together, although not as pronounced as in vivo, $CD44^{-/-}$ cells were impaired in their migration in vitro and this was independent of adhesion to the substrate.

An alternative explanation for the effects of CD44 could be that it regulates cellular polarity. In fact, CD44 enhances anterior-posterior asymmetry in neutrophils in response to chemokines in vitro (Alstergren et al., 2004). To address this possibility, we performed cell-shape analysis of CTL. We classified CTL based on 3 cellular shapes: round, and extended with or without a uropod (Figure 3E). Comparison of the frequency of round versus extended shapes revealed similar values in both groups, suggesting that CD44-deficient cells retain their capacity to break radial symmetry (Figure 3F). However, CD44-deficient cells showed significantly reduced efficiency to form uropods (Figure 3G), indicating that CD44 may promote migration by supporting cellular polarity.

Based on the finding that $CD44^{-/-}$ cells exhibited diminished uropod formation, but that nevertheless most of these cells were actively migrating (at reduced speed and displacement), we speculated that the lack of CD44 might impair sustenance of a polarized shape. To test this possibility, we developed a shape-change assay to measure the robustness of a sustained polarized phenotype of CTL. Thus, we counted the frequency of switches between a non-polarized (round) and polarized (extended) shape on cells cultured in plastic dishes. Round wildtype cells that developed an extended shape usually retained their shape throughout the observation period, corresponding to a switch rate of 1 (Figures 3H-3J; Movie S5A). In contrast, round knock-out cells that extended their shape frequently switched back to a round shape, a cycle that was often repeated multiple times. Thus, there was a significant increase in $CD44^{-/-}$ cells with switch rates equal to or greater than 2 (Figure 3J; Movie S5B)

In order to confirm that a similar phenomenon was happening in vivo, we determined the number of wildtype and $CD44^{-/-}$ OT-I T cells exhibiting uropods within EL4 tumors. Consistent with the in vitro results, we observed a significant decrease in uropod-containing cells within the $CD44^{-/-}$ population (Figure 3K). Together, these data indicate that the lack of CD44 leads to an impaired capacity of CTL to sustain mature polarization in the front-rear axis.

The intracellular domain (ICD) regulates membrane localization and promigratory effects of CD44

The results described so far suggested that the promigratory function of CD44 is due to a polarity-sustaining activity that occurs in the absence of ligand (HA) binding. To test whether

this deficiency could be rescued by CD44, we transduced CD44-deficient CTL with the full-length molecule. CD44-expression levels of transduced cells were similar to that of wildtype OT-I cells transduced with GFP-encoding control retrovirus (Figure S6). When placed on top of a collagen gel, CD44-transduced cells showed enhanced motility when compared with non-transduced (GFP^-) $CD44^{-/-}$ cells, or cells transduced with a vector that confers GFP but not CD44 expression (Figures 4A-4C).

To determine the functional domains important for promoting migration, we transduced $CD44^{-/-}$ CTL with mutant CD44, CD44ΔECD, containing a truncated extracellular domain of only 19 amino-acids, which lacks the HA-binding link-domain, and is therefore principally deficient in its receptor function (Peach et al., 1993) (Figure 4D). A second group of cells was transduced with CD44ΔICD containing a truncated cytoplasmic domain of only 7 cytoplasmic amino-acids, thereby lacking any functional adaptor domains (Figure 4D). A third group was transduced with full-length CD44 as a control (Figure 4D). Expression of CD44ΔECD had a pro-migratory effect similar to that of wildtype CD44 ($P>0.05$; Figure 4E). In contrast, cells expressing CD44ΔICD showed reduced motility versus full-length CD44- and CD44ΔECD-transduced cells ($P<0.001$), but equal motility as non-transduced cells or cells transduced with GFP-only vectors ($P>0.05$, Figure 4E).

To assess whether these effects might be due to changes in the subcellular organization of CD44 molecules, we generated retroviruses conferring expression of GFP-tagged CD44 proteins (Figure 4D). CD44-GFP proteins showed similar surface expression levels and promigratory function as the non-tagged correlates (Figure 4F and S7). As described previously, full-length CD44 was enriched at the uropod of polarized T cells (Sanchez-Madrid and del Pozo, 1999) (Figure 4G, red arrowheads). Consistent with the migration analysis, the ECD was dispensable to achieve this positioning (Figure 4G). In contrast, deficiency of ICD led to a redistribution of CD44 with punctate, cytoplasmic staining pattern in addition to some surface staining (Figure 4G). Together, these data provide evidence that the intracellular, but not the extracellular domain is important for the promigratory activity of CD44 in effector CTL.

The promigratory effect of the ICD is mediated by pERM recruitment to the plasma membrane

The ICD of CD44 contains an ERM binding domain. Phosphorylated ERM (pERM) has previously been shown to promote cell polarity and migration by its capacity to link the actin cytoskeleton to the membrane, and to assemble a membrane-targeted multi-molecular signaling complex (Bretscher et al., 2002). To address whether ERM members were involved in the effects of CD44 on mediating CTL polarity and migration, we determined the subcellular localization of pERM in wildtype and $CD44^{-/-}$ OT-I cells by immuno-fluorescence microscopy. 65% of wildtype cells revealed accumulation of surface-localized pERM (Figure 5A). In polarized cells, pERM showed a predilection to the uropod, correlating with the expression pattern of CD44 (Figure 5A, red arrow). In contrast, CD44-deficient cells showed a significant reduction in the capacity to induce localized accumulation of pERM (Figure 5A).

To further assess whether pERM interaction was responsible for CD44 recruitment to the uropod, we generated a deletion mutant, (CD44ΔERM-GFP), that specifically lacked the ERM binding domain (Yonemura et al., 1998). Flow cytometry revealed that surface expression of CD44ΔERM-GFP was similar to that of full-length CD44-GFP (Figure 5B). Using fluorescence microscopy, we determined that CD44ΔERM-GFP was strongly enriched at the membrane. However, in contrast to the asymmetric distribution of CD44-GFP in polarized cells, CD44ΔERM-GFP was distributed evenly on the membrane of OT-I cells (compare Figures 5C and 5D). Thus, the ERM-binding domain appears dispensable for the recruitment of CD44 to the plasma membrane, but plays a function in enriching CD44 to particular subregions. We then generated time-lapse movies of in vitro-cultured CTL expressing CD44-

GFP or CD44ΔERM-GFP. Strikingly, CD44-GFP accumulated at discrete membrane locations preceding the formation of a uropod (Movies S6A and S6C). This was followed by forward translocation of the cell body (Movies S6A and S6C). In contrast, CD44ΔERM-GFP failed to accumulate stably at specific sublocations resulting in frequent unstable shape changes of the cells with little to no forward propulsion (Movies S6B and S6D). Consequently, CD44ΔERM-GFP-expressing cells migrated significantly slower than those expressing full-length CD44 or CD44ΔECD-GFP ($P<0.001$), but similarly to cells expressing CD44ΔICD-GFP or GFP alone ($P>0.05$) (Figures 5E-5G). These data suggest that pERM recruitment to the ICD of CD44 stabilizes cell polarity, which in turn supports migration.

CD44 is critical for target cell screening efficiency of TIL

Having defined the migratory defect of $CD44^{-/-}$ effector CTL both in vitro and in vivo, it was important to determine the role of CD44 in interactions with target cells, one of the hallmark activities of cytotoxic T cells. One possibility is that the reduced interstitial migration of CD44-deficient T cells leads to a reduced capacity to screen the tissue for the presence of target cells. To test this hypothesis, we measured the frequency of tumor cell contacts by individual CTL that engaged in short-term (<10 minutes) interactions. We found that wild-type T cells detaching from a tumor cell after a short-term interaction typically succeeded in re-initiating interstitial migration, followed by subsequent interactions with several additional tumor cells (4.1±0.2 interactions during the observation period of 30 min; Figure 6A and 6B). In contrast, after terminating a short-term interaction, CD44-deficient cells exhibited cell shape changes that failed to translate into effective forward propulsion, leading to significantly reduced subsequent tumor cell encounters (1.5±0.2 interactions; $p<0.0001$; Figure 6A and 6B). The reduced capacity to screen for target cells was also reflected by prolonged time-periods that noninteracting CD44-deficient cells required to establish contacts with tumor cells (Figure 6C). This defect led to a pronounced increase in CD44-deficient TIL that failed to bind to any tumor cells during a 30 minute observation period (Figure 6D). These results provide direct evidence that the target cell screening efficiency is decreased in CD44-deficient T cells.

CD44 is dispensable for the quality of T lymphocyte interactions with target cells in vivo

We next determined the quality of cellular interactions once they were established by TIL. Previous evidence supports the importance of polarization in cellular interactions of CTL. For example, interference with the polarity network in CTL not only has profound effects on migration, but also on IS formation following TCR signals in CTL in vitro (Ludford-Menting et al., 2005), attesting to similar regulatory cues of these processes. We adoptively transferred graded numbers (2×10^6, 5×10^6, 2×10^7) of OT-I T cells into mice harboring E.G7-OVA-ECFP tumors (Mrass et al., 2006), and analyzed cellular interactions at different time points. Similar to what we found with OT-I CTL (Mrass et al., 2006), CD44-deficient OT-I cells underwent both transient and long-term interactions within E.G7-OVA tumors (Figures 6E and 6F; Movie S7). Strikingly, the duration of CD44-deficient cell interactions was indistinguishable from their wildtype counterparts (Figure 6F, Movie S7), indicating that CD44 is not involved in physical contacts of TIL. These results further suggest that facultative polarity in migrating and interacting T cells are molecularly distinct processes.

$CD44^{-/-}$ CTL are impaired in their tumor-rejecting activities

Together, our results show that $CD44^{-/-}$ lymphocytes exhibit a specific defect in interstitial migration and screening for target cells, but that they are still capable of recognizing target cells. This may not be so relevant during the early phase of tumor rejection, when the tumor bed is densely packed with tumor cells (Figure S8A), and CTL do not have to migrate over prolonged distances in order to find a target. However, at later stages (beginning on day 4 after adoptive transfer) tumor cells become less dense due to apoptosis (Figures S8B and S8C). At

this stage, TIL migration may be essential to detect and destroy target cells. In addition, at high T cell frequency within tumors the consequence of a migratory defect may not be as apparent as when T cells are present at low densities, because the likelihood of tumor-cell-encounters would be higher in the former scenario.

In order to test this prediction, we measured the growth of tumors in mice bearing E.G7-OVA tumors that received graded doses of wildtype or $CD44^{-/-}$ antigen-specific OT-I CTL. Irrespective of their CD44-status, CTL initially induced regression of growing tumors. This effect was more pronounced when higher numbers of CTL were transferred (Figure 7A). Strikingly, beginning 4 days after CTL transfer, the efficacy of CD44-deficient CTL to induce tumor shrinkage was reduced (Figures 7A and 7B). Particularly at lower T cell numbers, this led to an accelerated re-occurrence of tumors in the $CD44^{-/-}$group (Figures 7A and 7B). The percentage of large tumors (>100 mm^3) was significantly higher in mice receiving knockout CTL (Figures 7C and 7D). Together, this resulted in increased mortality of the mice in the $CD44^{-/-}$ CTL group (Figure 7E).

In order to exclude that the failure of $CD44^{-/-}$ T lymphocytes to permanently reject tumors was due to a difference in survival as compared to wildtype cells, we determined the number of cells accumulating in EL4 tumors and the spleen in a time course (Figure 7F and data not shown). These experiments showed that $CD44^{-/-}$ T cells persisted to the same extent as their wildtype counterparts for at least 9 days after adoptive transfer. In addition, we counted wildtype OT-I cells in three individual E.G7-OVA tumors that were not rejected. We found that there were identical numbers of wildtype and $CD44^{-/-}$ CTL in these tumors (data not shown).

In summary, these results indicate that CD44 is an important determinant of the tumor-rejecting capability of TIL, most likely relating to the pro-migratory effects of this molecule.

Discussion

Cellular polarity is a hallmark of two main activities of killer T lymphocytes, locomotion through tissue stroma and physical interactions with target cells. The results in the present paper provide insight into the molecular basis of polarity formation in CTL directly within the intact tumor microenvironment. We found that interference with sustained polarity resulting from CD44-deficiency decreases the capability of these cells to migrate through the effector site, but does not impact on the stability of interactions with target cells. Thus, our study demonstrates that facultative polarity established during migration and cellular interactions are molecularly distinct processes. In addition, we show that the fine-tuning of killer T cell navigation through the interstitial space is essential for efficient screening for tumor cells, which in turn leads to efficient tumor cell surveillance.

The capability to rapidly migrate to any site in the body is a defining feature of T cells, which ensures that they detect and destroy target cells. Several distinct migratory checkpoints regulate the appropriate targeting of T cells into peripheral tissues. In the initial step, T lymphocytes enter organs from the blood stream, which is achieved by a cascade of specific molecular interactions with the vascular endothelium culminating in firm lymphocyte adhesion [reviewed in (Springer, 1994)]. In the second step, adherent T cells transmigrate through the vascular wall eventually reaching the interstitial space of target organs. Finally, after entering the tissue stroma, T cells crawl through the extracellular matrix, thus presumably facilitating the screening for cells presenting cognate antigen on their surface. The molecular and biophysical cues underlying the first two steps have been studied in great detail both in vitro and in vivo. Our data clearly demonstrate that interstitial effector T cell migration is an additional checkpoint whose tight regulation is important for the effectiveness of the immune response.

Our study shows that CD44 regulates T cell locomotion through the tumor stroma, but not trafficking of CTL to tumors. While it has been known for a long time that CD44 expression is strongly induced in T cells by TCR signals, its precise role in T cell function has remained incompletely understood. Previous studies have found that CD44 is involved in homing of T lympocytes to sites of inflammation, probably via mediating interaction of blood-borne T cells with the endothelial wall (DeGrendele et al., 1997). Nevertheless, in our experiments CTL homed effectively into subcutaneous tumors, irrespective of their CD44-status. In their original study, de Grendele *et al*. used short-term in vivo-activated $CD4^+$ T cells with high HA-binding activity for their homing experiments (DeGrendele et al., 1997). Consistent with previous data assessing HA-binding to T cells during immune responses (Lesley et al., 1994), we found that terminally differentiated CTL showed high CD44 expression but no HA-binding capacity. Therefore, it appears that CD44 may have an early, transient function in the homing process of T cells into peripheral sites, while at later timepoints it is dispensable for T cell trafficking.

To better understand T cell activities in the extravascular space, we made use of time-lapse two-photon microscopy. Recently, this technology has been used to unravel the cellular dynamics and anatomical context of T cell migration in intact tissues. Thus, it has been shown that, in the absence of cognate antigen, naïve T cells in peripheral lymph nodes migrate very actively and in random directions, a process partially dependent on chemokine signals (Miller et al., 2002; Worbs et al., 2007). While naïve T cells appear to use the fibroblastic reticular cell network as a migratory guidance cue (Bajenoff et al., 2006), the molecules mediating these interactions are unknown. In contrast to LN, tumors do not contain an organized FRC network. Nevertheless, the ECM at these sites is rich in HA and collagen fibers (Condeelis and Segall, 2003; Knudson, 1996; Ricciardelli and Rodgers, 2006; Zalatnai, 2006), and our previous observation that migrating TIL underwent intimate interactions with ECM fibers (Mrass et al., 2006) suggested that these structures may serve similar purposes for CTL as the FRC network does for naive T cells.

On the other hand, it has been proposed that leukocytes undergo only transient or no firm adhesion with the substrate both in 3D models in vitro and in tissues in vivo. Thus, it has been suggested that lymphocytes extend cell protrusions into tissue-pockets to generate mechanical traction (Schor et al., 1983). This process has been dubbed “biophysical migration”, and may explain why leukocytes migrate >100 fold faster than epithelial/mesenchymal cells (Friedl et al., 2001). Recent evidence has shown that leukocyte migration in 3D collagen gels is completely independent of integrins, but rather relies on the force generated by actin network expansion (Lammermann et al., 2008). Our data extend this notion as they suggest that the ECD of CD44 is dispensable for migration of activated T cells in vitro, while the ICD is sufficient to restore normal migration in $CD44^{-/-}$ cells. This indicates that the effect of CD44 in CTL may be independent of ligand binding in situ, which is further substantiated by the inactive, i.e. HA non-binding, state of the molecule on TIL isolated from tumors.

While $CD44^{-/-}$ CTL showed normal adhesive function towards ECM components in vitro, they were deficient in formation of a mature polarized cell shape, evidenced by the reduced presence of uropods in migrating cells both in vitro and in vivo. CD44 does not appear to be required for the initiation of polarity, i.e. symmetry-breaking, as other molecules such as Scribble (Ludford-Menting et al., 2005). Rather, it seems to function as a polarity stabilizer, shown by shape change assays of migrating CTL. In contrast to the requirement of CD44 in the regulation of polarity during migration, $CD44^{-/-}$ CTL interacted with tumor cells similarly to wildtype T lymphocytes. This is consistent with the observation that, morphologically, interacting wildtype (and $CD44^{-/-}$) TIL did not reveal clearly formed uropods, but were usually of round shape. Therefore, we propose that the main function of CD44 in T lymphocytes within the interstitial space is the organization of cell shape during active migration.

At the molecular level, upon ligand binding, the cyoplasmic domain of CD44 has been shown to recruit a number of molecules, including ERM family members, ankyrin, small Rho GTPases, and tyrosine kinases, thereby transducing signals from the cell surface to the cytoskeleton (Bretscher et al., 2002; Ponta et al., 2003; Turley et al., 2002). Several of these pathways have been proposed to mediate the promigratory effects of CD44. In vitro experiments have indicated the involvement of ERM molecules in the regulation of directional migration of fibroblasts and melanoma cells after exposure to chemokines (Legg et al., 2002). However, despite mapping of the ERM-binding domain to a short amino-acid stretch at the intracellular domain of CD44, and the description of a point mutation within this domain that interferes with chemotaxis in a dominant-negative manner, the precise function of the ERM-binding domain in the effects of CD44 on T cell behavior has been unknown (Legg et al., 2002; Ponta et al., 2003). Our results provide genetic evidence that recruitment of pERM to the CD44 ICD is required for the promigratory effect of CD44 in CTL. CD44 promotes enrichment of pERM at the membrane, and reciprocally, interaction with pERM is required for CD44 to become polarized at the membrane. It is likely that after recruitment to the membrane, pERM crosslinks the actin cytoskeleton, leading to the localized enrichment of the CD44-pERM complex. Our data are consistent with a recent study in a thymoma cell line showing that a pERM supports polarity by the assembly of a molecular complex supporting “posteriority” (Lee et al., 2004).

The fact that CD44-deficient CTL exhibit a specific defect in interstitial migration, while all other investigated properties, including homing, cytotoxicity, and cytokine production remain fully functional, suggests that migration is indeed an integral part of the function of CTL. Nevertheless, it is worthwhile to note that at very early time-points, where the tumor-tissue is still packed with target cells (i.e. up to day 3 after adoptive transfer), the effects of $CD44^{-/-}$ CTL were comparable to wildtype cells. Thus, initially, rejection of tumors was induced to a similar extent. In contrast, beginning on day 4 after adoptive transfer, CD44-deficient cells showed a substantial decrease in their anti-tumor effect. Under these conditions, the density of target cells is reduced, and a large fraction of the tumor volume is comprised of inflammatory cells and dead tumor cells. We speculate that optimal interstitial migration is required at the later phase of tumor rejection, which is based on the sufficient detection of target cells within the tumor bed. Hence, if CTL locomotion is disturbed at this time point, residual tumor cells have the chance to escape immuno-surveillance resulting in early re-occurrence of overt cancer. Together, these results indicate an early and late phase in tumor destruction, defined by the migratory properties of effector T cells and regulated by CD44.

Experimental procedures

Mice

Mouse strains included DPE^{GFP} mice, in which GFP is expressed by all T cells, TCR-transgenic OT-I mice, and OT-I$xDPE^{GFP}$ mice (Mempel et al., 2006; Mrass et al., 2006). $CD44^{-/-}$ mice, crossed to the C57BL/6 background for >10 generations, were bred with OT-I or OT-I$xDPE^{GFP}$ strains. C57BL/6 wildtype mice were obtained from Charles River Laboratories. All experimental protocols including animals were approved by the Institutional Animal Care and Use Committee of The Wistar Institute.

Two-photon microscopy of tumors and imaging analysis

Tumor tissue preparation was carried out as described previously (Mrass et al., 2006). Briefly, tumors were explanted and placed in an imaging chamber. Superfusion with prewarmed and oxygenated medium was carried out throughout the experiment to maintain tissue viability. Two-photon microscopy and imaging analysis was carried out on a Prairie Technology Ultima System equipped with a 40× (NA 0.8) water immersion objective in combination with a diode-

pumped, wideband mode–locked Ti:Sapphire femtosecond laser (Coherent Chameleon). Tissues were exposed to laser light at a wavelength of 900 nm. Appropriate filter sets were used to specifically detect light emitted due to second harmonic generation or by the excited fluorophores. 3D image stacks were transformed into movies using Volocity software (Improvision). Mean migration velocities, cellular displacement, and confinement ratios (total length of track divided by distance between starting and end point) as well as turning angles and instantaneous velocity were calculated as described (Mrass et al., 2006).

In vitro T cell migration assay

A collagen suspension (1 mg ml^{-1}) was diluted 1:5 in PBS/0.2% bovine serum albumin. 100 μl of this solution were placed in 96 well plates, and solidified for 2 to 16 hours at room temperature. Alternatively, fibronectin (10 μg ml^{-1}) was used to coat plates. 10^5 OT-I effector T cells in prewarmed media (100 μl) supplemented with IL-2 (20 ng ml^{-1}) were added. After the cells settled, they were imaged with fluorescence and phase contrast microscopy (Nikon TE300 microscope) to capture and distinguish cells with and without fluorescent tag. Time-lapse sequences of 10’30” duration with one frame captured every 30 seconds were generated. T cell motility parameters were analyzed using Volocity software and calculated as described for intact tissues.

Statistical methods

Unless indicated otherwise, Mann Whitney test was used for comparisons of two groups. Kruskal-Wallis followed by Bonferroni test was used for comparisons of more than two groups. The chi-square test was used for the comparison of categorical data. KS normality test and D’Agostino & Pearson omnibus normality test were employed when using assays that require normal distribution. A difference was considered significant if $P<0.05$. The error bars in all charts represent standard errors of the mean.

Supplementary Material

Refer to Web version on PubMed Central for supplementary material.

Acknowledgments

We thank Dr. M. Fukunaga-Kalabis and Dr. A. Iparraguirre-Wolf for helpful discussion, and Drs. E.J. Wherry and M. Herlyn (all at the Wistar Institute) for providing reagents. S.L.R. and E.P. were supported by grants from the NIH. W.W. was supported by NHMRC grant 512265 and a Life Sciences Award from the NSW government. P.M. is the recipient of a Cancer Research Institute fellowship.

References

Alstergren P, Zhu B, Glogauer M, Mak TW, Ellen RP, Sodek J. Polarization and directed migration of murine neutrophils is dependent on cell surface expression of CD44. Cell Immunol 2004;231:146–157. [PubMed: 15919379]

Bajenoff M, Egen JG, Koo LY, Laugier JP, Brau F, Glaichenhaus N, Germain RN. Stromal cell networks regulate lymphocyte entry, migration, and territoriality in lymph nodes. Immunity 2006;25:989–1001. [PubMed: 17112751]

Bousso P, Robey EA. Dynamic behavior of T cells and thymocytes in lymphoid organs as revealed by two-photon microscopy. Immunity 2004;21:349–355. [PubMed: 15357946]

Bretscher A, Edwards K, Fehon RG. ERM proteins and merlin: integrators at the cell cortex. Nat Rev Mol Cell Biol 2002;3:586–599. [PubMed: 12154370]

Cahalan MD, Parker I. Choreography of cell motility and interaction dynamics imaged by two-photon microscopy in lymphoid organs. Annual review of immunology 2008;26:585–626.

Cahalan MD, Parker I, Wei SH, Miller MJ. Two-photon tissue imaging: seeing the immune system in a fresh light. Nat Rev Immunol 2002;2:872–880. [PubMed: 12415310]

Chang JT, Palanivel VR, Kinjyo I, Schambach F, Intlekofer AM, Banerjee A, Longworth SA, Vinup KE, Mrass P, Oliaro J, et al. Asymmetric T lymphocyte division in the initiation of adaptive immune responses. Science 2007;315:1687–1691. [PubMed: 17332376]

Condeelis J, Segall JE. Intravital imaging of cell movement in tumours. Nat Rev Cancer 2003;3:921–930. [PubMed: 14737122]

DeGrendele HC, Estess P, Siegelman MH. Requirement for CD44 in activated T cell extravasation into an inflammatory site. Science 1997;278:672–675. [PubMed: 9381175]

Dustin ML. T-cell activation through immunological synapses and kinapses. Immunological reviews 2008;221:77–89. [PubMed: 18275476]

Friedl P, Borgmann S, Brocker EB. Amoeboid leukocyte crawling through extracellular matrix: lessons from the Dictyostelium paradigm of cell movement. J Leukoc Biol 2001;70:491–509. [PubMed: 11590185]

Germain RN, Miller MJ, Dustin ML, Nussenzweig MC. Dynamic imaging of the immune system: progress, pitfalls and promise. Nat Rev Immunol 2006;6:497–507. [PubMed: 16799470]

Halin C, Rodrigo Mora J, Sumen C, von Andrian UH. In vivo imaging of lymphocyte trafficking. Annual review of cell and developmental biology 2005;21:581–603.

Jacobelli J, Andres PG, Boisvert J, Krummel MF. New views of the immunological synapse: variations in assembly and function. Current opinion in immunology 2004;16:345–352. [PubMed: 15134784]

Knudson W. Tumor-associated hyaluronan. Providing an extracellular matrix that facilitates invasion. Am J Pathol 1996;148:1721–1726. [PubMed: 8669457]

Krummel MF, Macara I. Maintenance and modulation of T cell polarity. Nat Immunol 2006;7:1143–1149. [PubMed: 17053799]

Lammermann T, Bader BL, Monkley SJ, Worbs T, Wedlich-Soldner R, Hirsch K, Keller M, Forster R, Critchley DR, Fassler R, Sixt M. Rapid leukocyte migration by integrin-independent flowing and squeezing. Nature 2008;453:51–55. [PubMed: 18451854]

Lee JH, Katakai T, Hara T, Gonda H, Sugai M, Shimizu A. Roles of p-ERM and Rho-ROCK signaling in lymphocyte polarity and uropod formation. J Cell Biol 2004;167:327–337. [PubMed: 15504914]

Legg JW, Lewis CA, Parsons M, Ng T, Isacke CM. A novel PKC-regulated mechanism controls CD44 ezrin association and directional cell motility. Nat Cell Biol 2002;4:399–407. [PubMed: 12032545]

Lesley J, Howes N, Perschl A, Hyman R. Hyaluronan binding function of CD44 is transiently activated on T cells during an in vivo immune response. J Exp Med 1994;180:383–387. [PubMed: 7516415]

Lesley J, Kincade PW, Hyman R. Antibody-induced activation of the hyaluronan receptor function of CD44 requires multivalent binding by antibody. European journal of immunology 1993;23:1902–1909. [PubMed: 7688309]

Ludford-Menting MJ, Oliaro J, Sacirbegovic F, Cheah ET, Pedersen N, Thomas SJ, Pasam A, Iazzolino R, Dow LE, Waterhouse NJ, et al. A network of PDZ-containing proteins regulates T cell polarity and morphology during migration and immunological synapse formation. Immunity 2005;22:737–748. [PubMed: 15963788]

Mempel TR, Pittet MJ, Khazaie K, Weninger W, Weissleder R, von Boehmer H, von Andrian UH. Regulatory T cells reversibly suppress cytotoxic T cell function independent of effector differentiation. Immunity 2006;25:129–141. [PubMed: 16860762]

Miller MJ, Wei SH, Parker I, Cahalan MD. Two-photon imaging of lymphocyte motility and antigen response in intact lymph node. Science 2002;296:1869–1873. [PubMed: 12016203]

Mrass P, Takano H, Ng LG, Daxini S, Lasaro MO, Iparraguirre A, Cavanagh LL, von Andrian UH, Ertl HC, Haydon PG, Weninger W. Random migration precedes stable target cell interactions of tumor-infiltrating T cells. J Exp Med 2006;203:2749–2761. [PubMed: 17116735]

Mrass P, Weninger W. Immune cell migration as a means to control immune privilege: lessons from the CNS and tumors. Immunol Rev 2006;213:195–212. [PubMed: 16972905]

Ng LG, Mrass P, Kinjyo I, Reiner SL, Weninger W. Two-photon imaging of effector T-cell behavior: lessons from a tumor model. Immunological reviews 2008;221:147–162. [PubMed: 18275480]

Peach RJ, Hollenbaugh D, Stamenkovic I, Aruffo A. Identification of hyaluronic acid binding sites in the extracellular domain of CD44. J Cell Biol 1993;122:257–264. [PubMed: 8314845]

Ponta H, Sherman L, Herrlich PA. CD44: from adhesion molecules to signalling regulators. Nat Rev Mol Cell Biol 2003;4:33–45. [PubMed: 12511867]

Pure E, Cuff CA. A crucial role for CD44 in inflammation. Trends Mol Med 2001;7:213–221. [PubMed: 11325633]

Ricciardelli C, Rodgers RJ. Extracellular matrix of ovarian tumors. Semin Reprod Med 2006;24:270–282. [PubMed: 16944424]

Sanchez-Madrid F, del Pozo MA. Leukocyte polarization in cell migration and immune interactions. Embo J 1999;18:501–511. [PubMed: 9927410]

Schor SL, Allen TD, Winn B. Lymphocyte migration into three-dimensional collagen matrices: a quantitative study. J Cell Biol 1983;96:1089–1096. [PubMed: 6833393]

Shaw AS. T-cell activation and immunologic synapse. Immunologic research 2005;32:247–252. [PubMed: 16106076]

Springer TA. Traffic signals for lymphocyte recirculation and leukocyte emigration: the multistep paradigm. Cell 1994;76:301–314. [PubMed: 7507411]

Stinchcombe JC, Griffiths GM. The role of the secretory immunological synapse in killing by CD8+ CTL. Semin Immunol 2003;15:301–305. [PubMed: 15001168]

Turley EA, Noble PW, Bourguignon LY. Signaling properties of hyaluronan receptors. J Biol Chem 2002;277:4589–4592. [PubMed: 11717317]

Worbs T, Mempel TR, Bolter J, von Andrian UH, Forster R. CCR7 ligands stimulate the intranodal motility of T lymphocytes in vivo. J Exp Med 2007;204:489–495. [PubMed: 17325198]

Yonemura S, Hirao M, Doi Y, Takahashi N, Kondo T, Tsukita S, Tsukita S. Ezrin/radixin/moesin (ERM) proteins bind to a positively charged amino acid cluster in the juxta-membrane cytoplasmic domain of CD44, CD43, and ICAM-2. J Cell Biol 1998;140:885–895. [PubMed: 9472040]

Zalatnai A. Molecular aspects of stromal-parenchymal interactions in malignant neoplasms. Curr Mol Med 2006;6:685–693. [PubMed: 17022738]

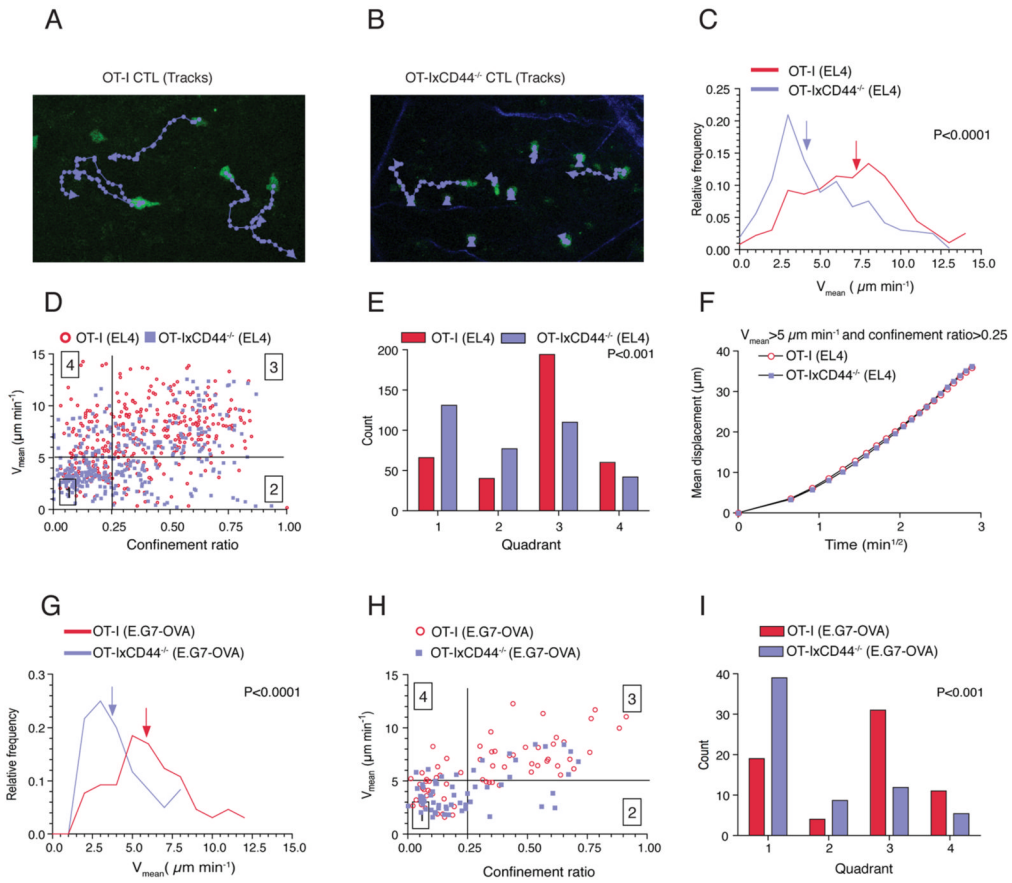

Figure 1. CD44 regulates the navigation of killer T cells through the tumor microenvironment

(A-F) C57BL/6 mice were injected s.c. with EL4-cells (10^6) not expressing cognate antigen for OT-I T cells. After the tumors became palpable, CTL (2×10^7) at day 8 of stimulation generated from OT-IxDPE^{GFP} or OT-IxCD44$^{-/-}$xDPE^{GFP} were adoptively transferred through the tail-vein. Three days later, the tumors (n=14) were explanted and subjected to two-photon microscopy. T cells were tracked and analyzed. (A, B) Representative tracks of migrating T cells (8'45"). (C) The distribution of the mean velocity of individual tracks is plotted. Arrows indicate the median velocity. (D) Individual tracks of migrating cells were plotted according to their confinement ratio and mean velocity. Quadrants were set to distinguish 4 populations of cells. Symbols represent tracks of individual cells. (E) The distribution of the individual tracks within the 4 quadrants shown in (D) is depicted. (F) A square root of time versus displacement plot was calculated from the tracks in quadrant 3.

(G-I) As in (C-E) except that mice were injected with E.G7-OVA tumors (n=3) instead of EL4 tumor cells and that two-photon imaging was carried out 4 days after adoptive transfer.

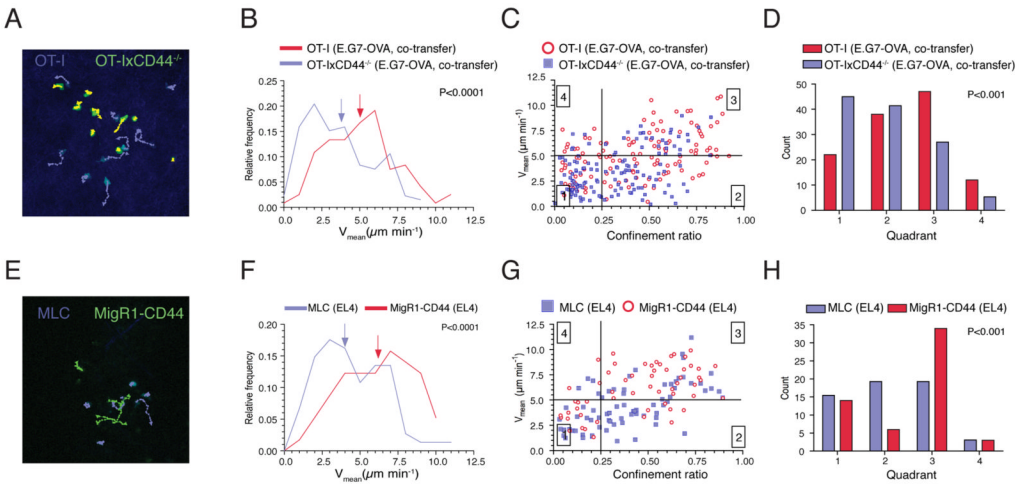

Figure 2. Direct regulation of TIL motility by CD44

(A-D) E.G7-OVA tumor bearing mice (as in Figure 1) were co-injected i.v. with 1.5×10^7 ECFP-OT-I and YFP-OT-IxCD44$^{-/-}$ CTL. Tumors (n=5) were explanted on day 4 after adoptive transfer. Two-photon imaging of ECFP$^+$ and YFP$^+$ cells and cell tracking analysis was carried as in Figure 1.

(E-H) OT-IxCD44$^{-/-}$ CTL transduced with ECFP alone or CD44-IRES-GFP (1.5×10^7 cells each) were adoptively transferred into EL4 tumor bearing mice. Tumors (n=2) were explanted on day 3 after adoptive transfer. Two-photon imaging of ECFP$^+$ and GFP$^+$ cells and cell tracking analysis was carried out as in Figure 1.

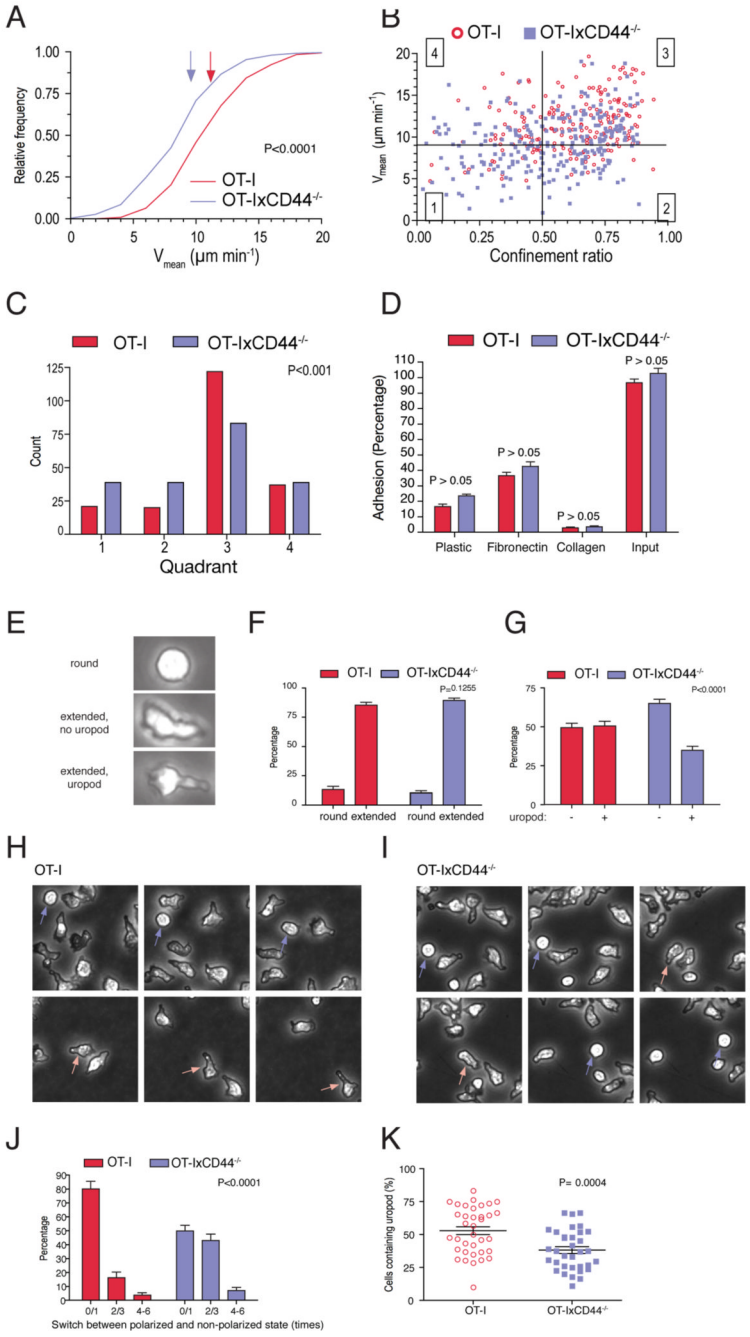

Figure 3. CD44 promotes polarity of effector CTL in vitro and in vivo

(A-C) CTL generated from OT-I or OT-IxCD44$^{-/-}$ mice at day 8 of culture were placed on top of a collagen gel. Using phase contrast microscopy, time-lapse sequences of the migratory behavior of the cells were generated. Frames were captured every 30 seconds for a period of 10.5 minutes. This was followed by tracking and data analysis as in Figure 1. Note that due to the faster migration velocities of T cells in vitro, gates in panel (B) were set differently for the cell culture experiments as compared to in vivo.

(D) T cell adhesion assay on 96 well plates uncoated or coated with collagen or fibronectin. Shown is the percentage of the adhering cells (n=32 wells for each condition in 4 independent experiments).

(E-G) CTL cultured on plastic-dishes were imaged with phase contrast microscopy. Cells were categorized and quantified according to their cell shape.
(H-J) Phase contrast microscopy was used to generate time-lapse sequences of CTL cultured on plastic dishes. The number of switches between round and extended shape was quantified (n= 81/67 OT-I/OT-IxCD44$^{-/-}$ cells). Indicated are the means of the percentages of switch-frequencies within individual time lapse-sequences (J, n=15 image sequences). Significance was tested using two-way ANOVA.
(K) The experiment was carried out as in Figure 1. Snapshots of time lapse videos generated in Figure 1 were taken, and the percentage of GFP^{+} cells containing uropods determined. Each symbol represents the value obtained in an individual region (4 independent experiments).

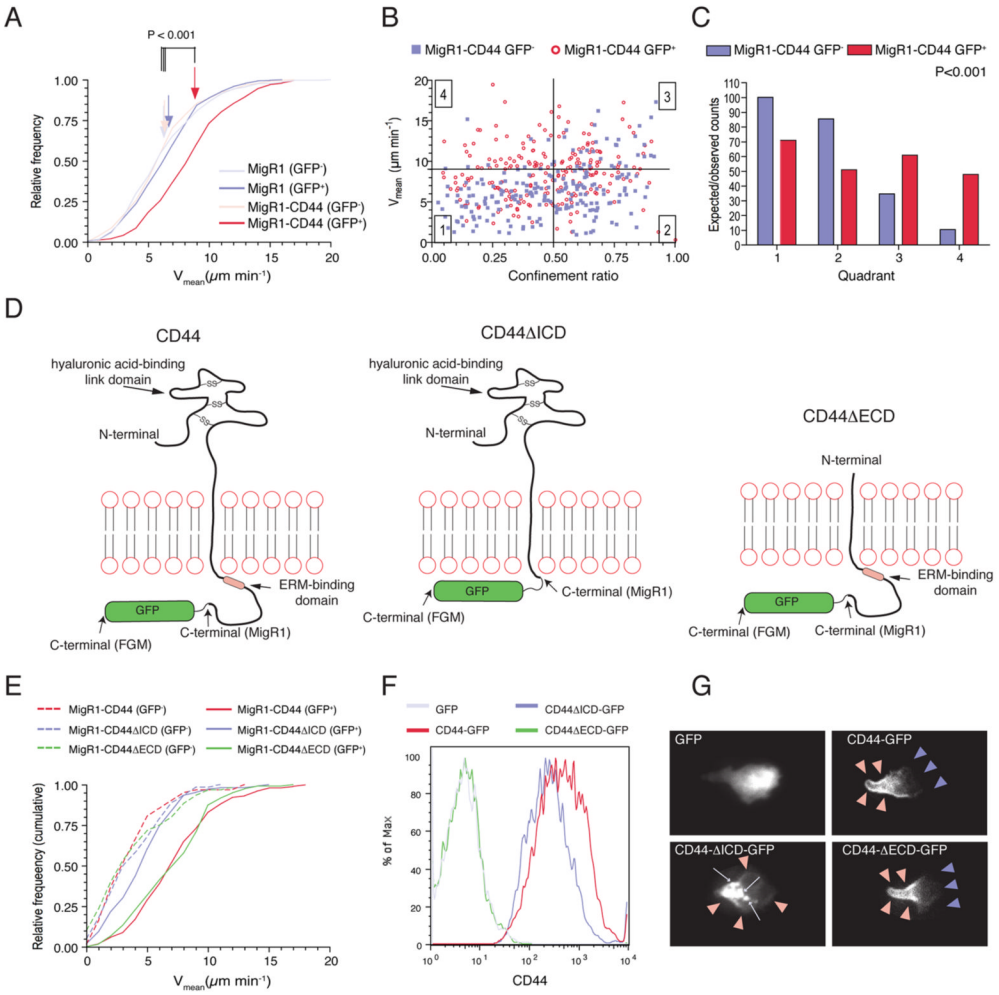

Figure 4. The intracellular domain of CD44 promotes T lymphocyte migration in vitro

(A-C) CTL generated from OT-IxCD44$^{-/-}$ mice were transduced with a retrovirus conferring expression of GFP and CD44 (MigR1-CD44) or GFP only (MigR1). Time-lapse sequences of CTL migrating on a collagen gel were captured simultaneously with phase-contrast and fluorescence microscopy to track GFP^{+} (transduced) and GFP^{-} (non-transduced) CTL, respectively. Data analysis was carried out as in Figure 1.

(D) Schematic representation of the different forms of CD44 used in the experiments.

(E) CTL generated from OT-IxCD44$^{-/-}$ mice were transduced with retrovirus conferring co-expression of GFP and the CD44 variants symbolized in (D). Migratory velocities were determined.

(F, G) CTL generated from OT-IxCD44$^{-/-}$ mice were transduced with FGM-retrovirus conferring expression of the CD44-GFP variants symbolized in (D). (F) CD44 expression on GFP^{+} cells was analyzed by flow cytometry. (G) Representative GFP^{+} T cells in the individual groups were captured with fluorescence microscopy.

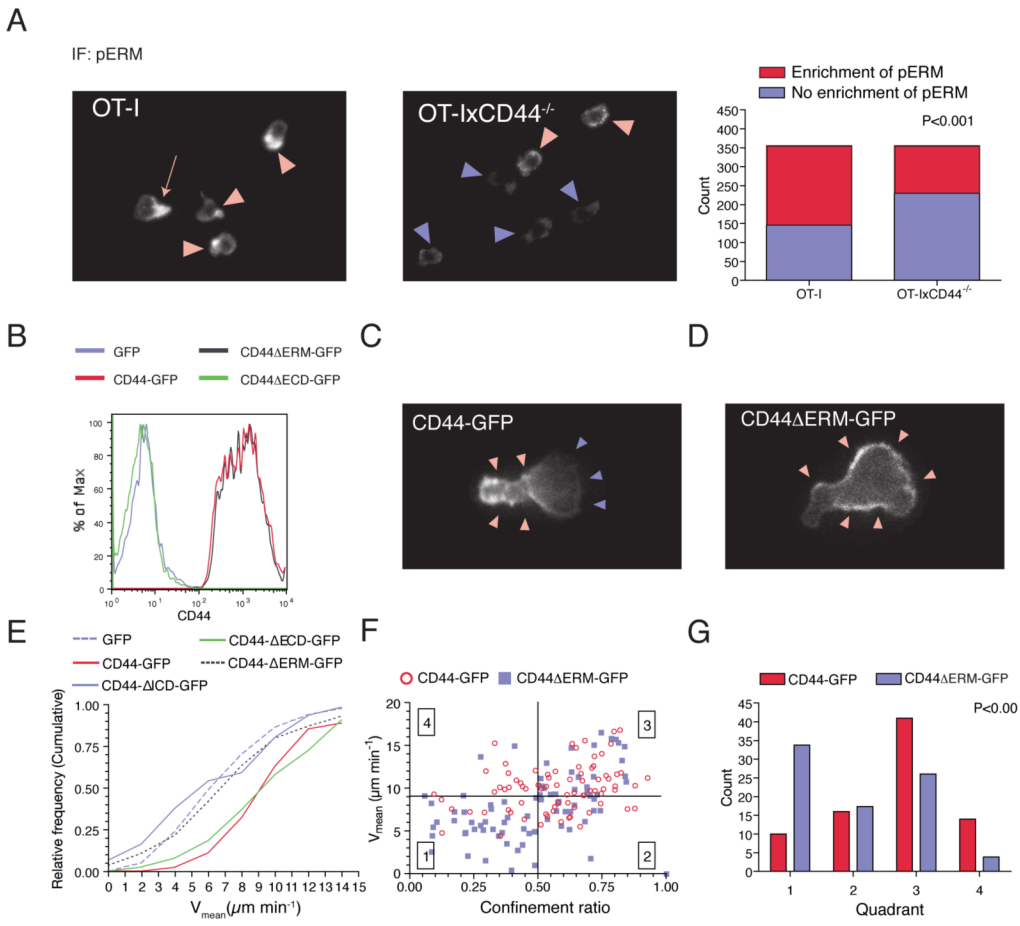

Figure 5. Recruitment of ERM is required for the promigratory effect of CD44 in killer T lymphocytes

(A) CTL were permeabilized and stained with mAb against pERM and analyzed by immunofluorescence microscopy. The percentage of cells with polarized localization of pERM was determined. Statistical significance was calculated using the Chi-Square test.

(B-G) CTL generated from OT-IxCD44$^{-/-}$ mice were transduced with a retrovirus conferring expression of the indicated CD44-GFP constructs. (B) CD44 expression on GFP^{+} cells was analyzed by flow cytometry. (C, D) Representative snapshots of in vitro cultured CTL transduced with CD44-GFP or CD44ΔERM-GFP. (E-G) The motility of CTL transduced with the indicated retroviral constructs on collagen gels was analyzed as in Figure 1.

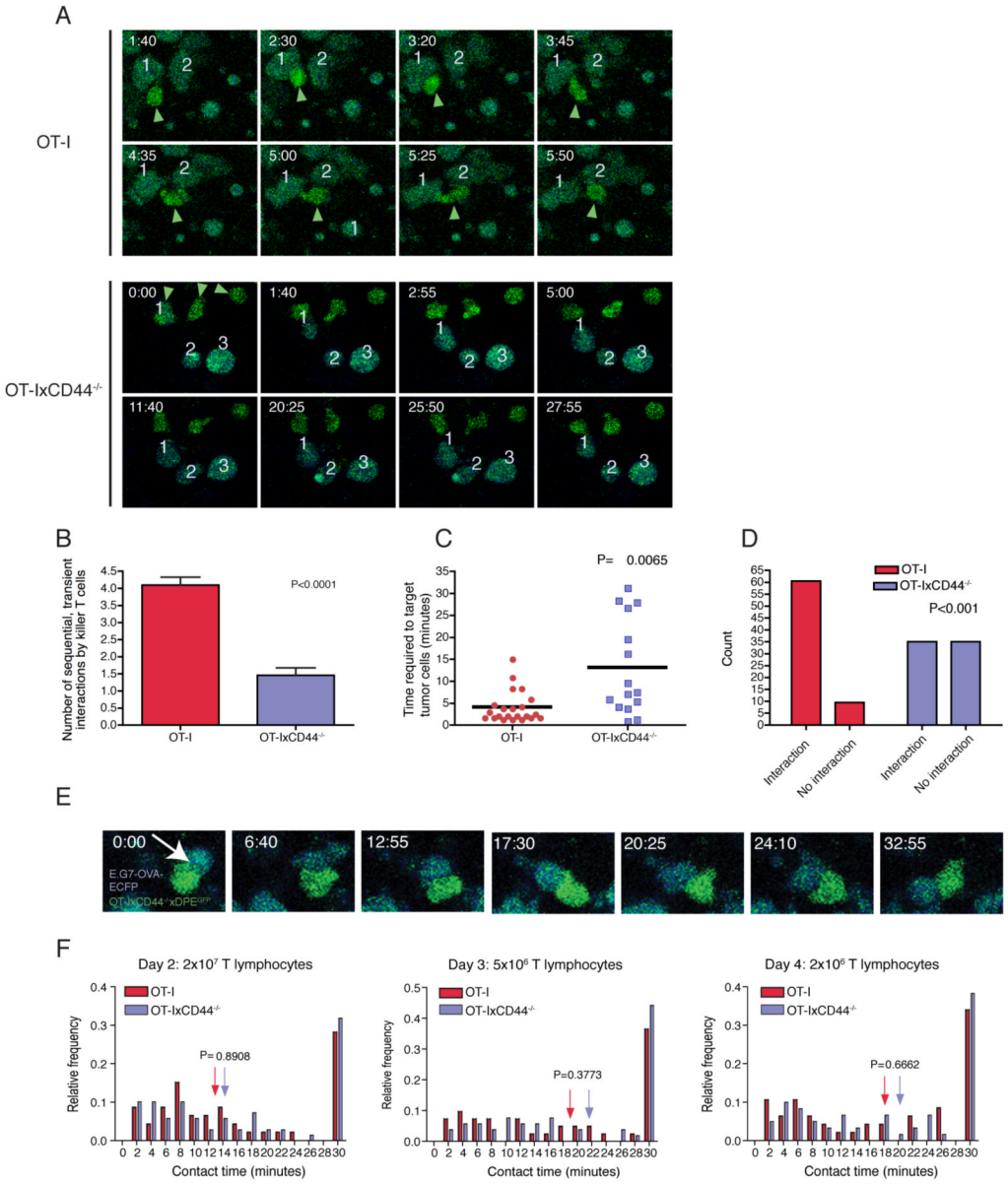

Figure 6. CD44 modulates target cell screening efficacy, but is not involved in physical interactions between killer T lymphocytes and tumor cells

C57BL/6 mice were injected subcutaneously into the flank with E.G7-OVA-ECFP tumor cells (10^6). After 9 days, 2×10^6, 5×10^6 or 2×10^7 CTL generated from OT-IxDPE^{GFP} or OT-IxCD44$^{-/-}$xDPE^{GFP} splenocytes were adoptively transferred. 2, 3 and 4 days later, the tumors were explanted and subjected to two-photon microscopy. (n=day 2, WT: 3 tumors, KO: 3 tumors; day 3, WT: 4 tumors, KO: 5 tumors; day 4, WT: 5 tumors, KO: 3 tumors for each T cell group).

(A) Snapshots from time-lapse sequences from mice that received 2×10^6 CTL are shown. CTL (green) are indicated with green arrowheads. Individual tumor cells are labeled with numbers to identify them throughout the observation period. The time is indicated in min:sec in the upper right corner of each panel.

(B) Tumor regions from mice that received 2×10^6 CTL were analyzed for the frequency of cellular interactions. Only CTL that could be tracked for 30 minutes, engaged in at least one

short-term interaction (<10 minutes) with a tumor cell and did not show any long-term interactions were included. The number of tumor cells that were targeted by these cells was counted. The data were generated from 3 independent experiments (WT: n=10 CTL; KO: n= 13).

(C) The areas analyzed in (B) were also analyzed for the time required for TIL to establish contacts with tumor cells. TIL that were not in contact with tumor cells were tracked until they made contact with a tumor cell. The elapsed time-period was measured and plotted.

(D) The areas analyzed in (B) were used to determine the number of TIL that succeed in establishing contacts with tumor cells. TIL were observed for a 30 minute time period. Cells that achieved contacts with at least 1 tumor cell were designated “interacting” cells, cells that failed to achieve contacts with any tumor cells were designated “non-interacting” cells. Shown is the number of interacting and non-interacting T cells.

(E) A representative long- term interaction between an OT-IxCD44$^{-/-}$ T cell and an E.G7-OVA-ECFP tumor cell is shown. The time is indicated in the upper left corner of each panel (minutes:seconds).

(F) The duration of interactions between E.G7-OVA-ECFP tumor cells and CD44-expressing or CD44-deficient CTL was measured (2×10^7: n=46/69 interactions; 5×10^6: n= 41/52 interactions; 2×10^6: n= 47/60 interactions).

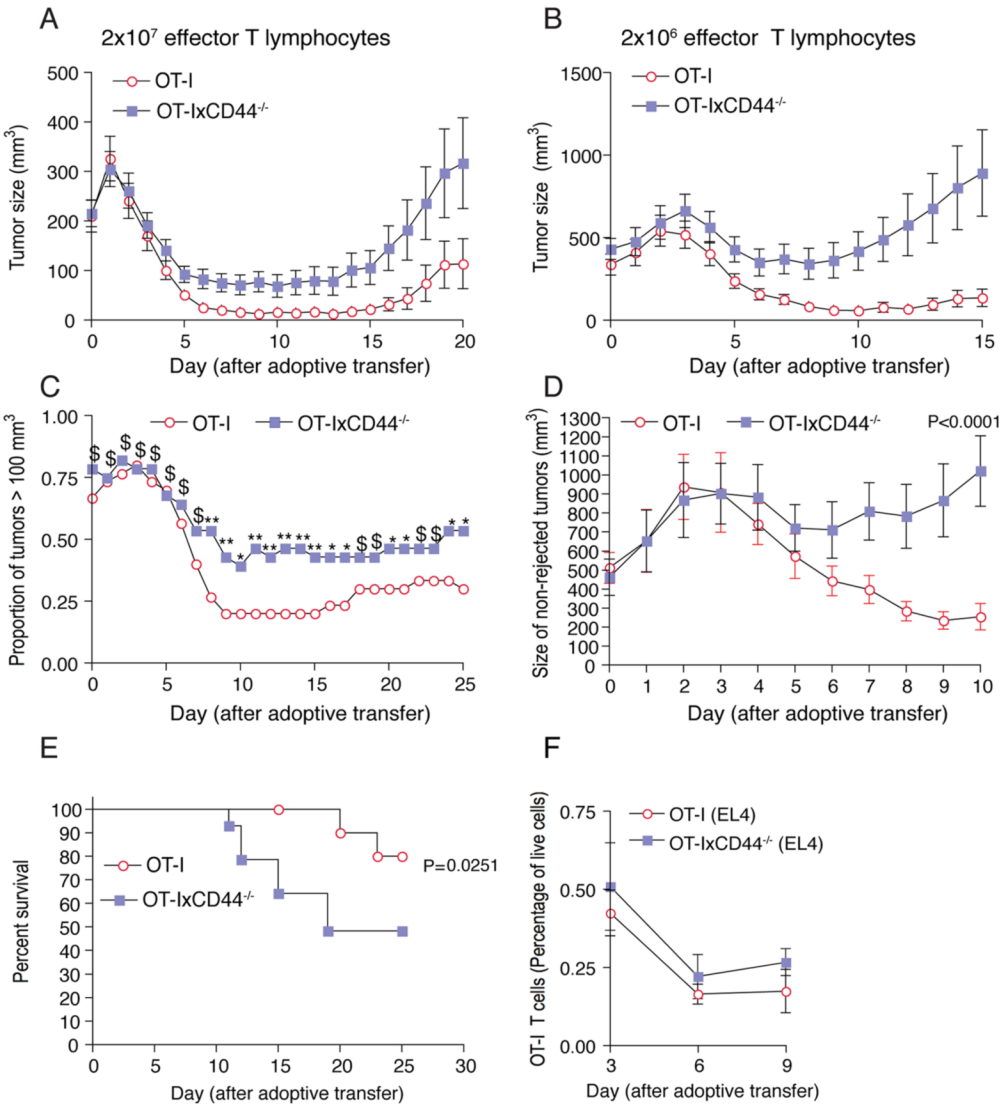

Figure 7. CD44 enhances the potency of the effector immune response

C57BL/6 mice were injected subcutaneously with E.G7-OVA cells (10^6). After 9-10 days, 2×10^7 (A) or 2×10^6 (B-E) CTL generated from OT-IxDPE^{GFP} or OT-IxCD44$^{-/-}$xDPE^{GFP} mice were adoptively transferred into tumor-bearing mice. (A) n=58 tumors for each T cell group; (B-E) n=30/28 tumors for OT-I and OT-IxCD44$^{-/-}$ CTL, respectively.

(A, B) The mean tumor volume was calculated for each group.

(C) The proportion of mice with tumors larger than 100 mm^3 after adoptive transfer is depicted. Chi-square test was used for each time point to determine if the proportion of rejected tumors in each group were different (**: P<0.005; *: P<0.05; $: P>0.1;).

(D) The mean volume only of tumors with a size larger than 100 mm^3 (day 10) was determined. Repeated measures two-way ANOVA was carried out to determine whether interaction occurs between the two curves (n=6/11 tumors).

(E) Survival curves of tumor-bearing mice that were treated with OT-IxDPE^{GFP} or OT-IxCD44$^{-/-}$xDPE^{GFP} T cells (n=15/14 mice) were determined.

(F) C56BL/6 mice were injected subcutaneously with EL4 tumor cells (10^6). At the indicated time-points single cell suspensions of the tumors were generated, and the number of OT-I and

OT-IxCD44$^{-/-}$ TIL were determined by flow cytometry (day 3: n=16/14 tumors; day 6: n=20 tumors; day 9: n=4 tumors).